Mathematical Model for the Bulk Polymerization of Styrene Using the Symmetrical Cyclic Trifunctional Initiator Diethyl Ketone Triperoxide. I. Chemical Initiation by Sequential Decomposition

E. Berkenwald,[1] C. Spies,[2] J. R. Cerna Cortez,[3] G. Morales,[3] D. Estenoz[1,2]

[1]Department of Chemical Engineering, Instituto Tecnológico de Buenos Aires (ITBA), Avenida Eduardo Madero 399, CP 1106, Buenos Aires, Argentina
[2]Instituto de Desarrollo Tecnológico para la Industria Química (INTEC), Universidad Nacional del Litoral, Consejo Nacional de Investigaciones Científicas y Técnicas (UNL/CONICET), Güemes 3450, CP 3000, Santa Fe, Argentina
[3]Centro de Investigaciones en Química Aplicada, Boulevard Enrique Reyna Hermosillo 140, CP 25253, Saltillo, México
Correspondence to: D. Estenoz (E-mail: destenoz@santafe-conicet.gov.ar) or G. Morales (E-mail: gmorales@ciqa.mx)

ABSTRACT: In this study, we experimentally and theoretically investigated the use of the symmetrical cyclic trifunctional initiator diethyl ketone triperoxide (DEKTP) in the bulk polymerization of styrene. The experimental study consisted of a series of isothermal batch polymerizations at different temperatures (120 and 130°C) with different initiator concentrations (0.005, 0.01, and 0.02 mol/L). A mathematical model was developed to predict the evolution of the reacting chemical species and the produced molecular weight distributions. The kinetic model included chemical and thermal initiation, propagation, transfer to the monomer, termination by combination, and reinitiation reactions. The simulation results predict the concentration of diradicals, monoradicals, and polymeric chains, characterized by the number of undecomposed peroxide groups. The experimental results showed that at reaction temperatures of 120–130°C, initiation by DEKTP produced an increase in the polymerization rates (R_p's) and average molecular weights, depending on the initiator concentration, due to sequential decomposition. The mathematical model was adjusted and validated with the experimental data. The theoretical predictions were in very good agreement with the experimental results. Also, an optimum initiator concentration was observed that achieved high R_p's and high molecular weights simultaneously. For polymerization temperatures of 120–130°C, the optimum concentration was 0.01 mol/L. © 2012 Wiley Periodicals, Inc. J. Appl. Polym. Sci. 000: 000–000, 2012

INTRODUCTION

The industrial use of multifunctional initiators in the bulk polymerization of styrene (St) has increased because of the possibility of obtaining high reaction rates and molecular weights simultaneously and enhanced mechanical properties in the product compared to those of polystyrene (PS) obtained with traditional initiators.[1–3]

The use of peroxide-type initiators is preferred over the use of azo or C—C initiators in the polymerization of vinyl monomers because of their relative ease of synthesis and lower rate of self-induced decomposition reactions.[4,5] However, the use of mono-functional initiators is limited because of the difficulty in obtaining an adequate balance between the reaction rate, molecular weight, polydispersity, and monomer conversion.[6,7]

In the last few decades, there has been growing interest in the industrial use of multifunctional initiators to avoid these limita-

tions. With the use of bifunctional initiators (with two reacting peroxide groups), it is possible for one to achieve the optimization of the polymerization processes while enhancing the final properties of the product (i.e., molecular weight, monomer conversion, and polydispersity).[1,2,7–10] Both symmetrical and asymmetrical initiators are used; this shows that it is possible, under the right temperature and initiator concentration, to obtain high reaction rates and high molecular weights simultaneously. The reaction temperature affects the thermal stability of peroxide groups, whereas the initiator concentration affects the polymerization rate (R_p) and reduces the polymerization time without lowering the molecular weight of the final product.[9]

A few researchers have theoretically studied the synthesis of PS with bifunctional initiators. Mathematical models were developed to predict the reacting species' concentrations and the molecular structure of the obtained polymer during the course of the polymerization reaction. Choi and Lei[1] and Kim et al.[3]

developed detailed kinetic models for the bulk St homopolymerization with symmetrical and asymmetrical diperoxyester initiators. They showed that at high temperatures, it is possible to obtain high reaction rates and molecular weights with relatively narrow molecular weight distributions (MWDs). Villalobos et al.[9] theoretically and experimentally investigated the polymerization of St with the following bifunctional initiators: 2,5-dimethyl-2,5-bis(2-ethylhexanol peroxy) hexane (Lupersol-256, L-256), 1,1-di(t-butyl peroxy) cyclohexane (Lupersol-331-80B), and 1,4-bis(t-butyl peroxycarbo) cyclohexane (D-162). Compared to the standard monofunctional case, bifunctional initiators reduce the polymerization time as much as 75% without substantial changes in the final product properties. In Estenoz et al.,[2] a detailed mathematical model was developed to simulate the synthesis of high-impact PS with symmetrical bifunctional initiators, such as L-256 and L-118 [2,5-dimethyl-2,5-bis(benzoyl peroxyl) hexane]. High reaction rates and high molecular weights were observed, and phase-inversion periods were produced at lower conversions.

There are a limited number of works dealing with the use of multifunctional initiators.[11–16] Cerna et al.[11] studied the bulk polymerization of St using initiators with different functionalities (monofunctional, difunctional, and trifunctional initiators). The particular case of initiation by diethyl ketone triperoxide (DEKTP), a cyclic trifunctional peroxide initiator, at 120–130°C yielded polymers with high molecular weights (250,000–450,000 g/mol, depending on the DEKTP concentration) at relatively short polymerization times (4–6 h). The obtained average molecular weights were higher than those obtained with the bifunctional initiator pinacolone diperoxide (PDP), which has a close molecular structure to that of DEKTP. In addition, the radical decomposition mechanism of DEKTP was found to be as complex as that of a linear bifunctional initiator, but DEKTP showed greater activity.[13] Two mechanisms have been proposed for the decomposition of DEKTP: a total decomposition of the three O—O groups at temperatures higher than 130°C and a sequential decomposition of the O—O groups at temperatures between 110 and 130°C. In the last case, Cerna et al.[11] were able to synthesize PS with undecomposed O—O in the polymer backbone.

In Scorah et al.,[14,15] the bulk polymerization of St and methyl methacrylate in the presence of the tetrafunctional initiator polyether tetrakis(tert-butylperoxy carbonate) (JWEB50) was experimentally and theoretically studied. The developed model allowed the calculation of monomer conversion, average molecular weights, and polymer structure and was validated with experimental results. Sheng et al.[16] studied the use of the cyclic trifunctional initiator 3,6,9-triethyl-3,6,9-trimethyl-1,4,7-triperoxonane in the bulk polymerization of St. The experimental results showed that it was possible to produce polymers with higher molecular weights and lower polydispersities at a higher rate. The obtained PS had O—O bonds in the molecular chains.

In this study, we dealt with the experimental and theoretical study of the DEKTP used in the bulk polymerization of St. A mathematical model was developed to predict the evolution of the reacting species' concentration, monomer conversion, and detailed polymer molecular structure. The effects of the reaction
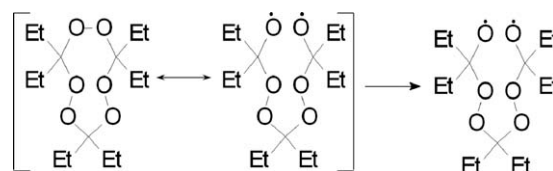

Figure 1. First stage of the sequential decomposition of DEKTP.

conditions on the process productivity and final product molecular characteristics were investigated.

EXPERIMENTAL

The DEKTP initiator was synthesized according to the following procedure:[17] in a 250-mL Erlenmeyer flask, 4.6 mL of hydrogen peroxide and 7.3 mL of sulfuric acid (70% v/v) were added, and the temperature was kept at −10°C. Then, 5.6 mL of diethyl ketone was added to the reaction medium, and the reaction was kept under agitation for 3 h. Thereafter, the organic phase was extracted with petroleum ether and dried with sodium sulfate for 12 h. The petroleum ether was removed under distillation, and the product was crystallized from methanol to yield a white powder.

Several bulk polymerizations of St were carried out in the presence of DEKTP at different temperatures and different initiator concentrations. In each experiment, a certain amount of DEKTP was dissolved in 2 mL of previously distilled St. The solution was placed in clean and dry test tubes, degassed by successive cycles of freezing and cooling from −180°C (with liquid nitrogen) to room temperature at reduced pressure. The tubes were sealed *in vacuo* and immersed in an oil bath. The selected polymerization temperatures were 120 and 130°C to ensure the sequential decomposition of the initiator molecule. Preliminary studies showed that at higher reaction temperatures (150–200°C), the decomposition mechanism of the initiator was no longer sequential and consisted of a simultaneous decomposition of all three peroxide groups.[18] The first stage in the sequential decomposition reaction for DEKTP is presented in Figure 1, where only one peroxide group of the DEKTP molecule suffers a decomposition reaction. Further stages of the sequential decomposition arise as the polymerization reaction generates polymer chains with undecomposed peroxide groups. The initiator concentrations were varied in the range 0.005–0.02 mol/L. The monomer conversion was determined gravimetrically, and the molecular weights were determined by gel permeation chromatography at different reaction times. The equipment used was a Hewlett-Packard HPLC 1050 instrument with software from Polymer Laboratories for Chemstation (manufactured by Agilent Technologies, Mexico City, Mexico). Refraction-index and UV detectors were used with ultrastyragel columns (10^5, 10^4, and 10^3 A). PS standards (580–3,900,000 g/mol) were used at ambient temperature. To measure conversion, the obtained polymer was directly precipitated in methanol (volume ratio = 1:10) and was filtered and dried *in vacuo* until a constant weight was reached (ca. 24 h).

The experimental results are presented in Table I and Figures 2 and 3. It can be observed that initiation by DEKTP allowed for high reaction rates and high average molecular weights simultaneously. As expected, increasing the initiator concentration

Table I. Experimental Results and Theoretical Predictions for the Bulk Polymerizations of St in the Presence of DEKTP

Experiment no.	T (°C)	$[I^{(3)}]$ (mol/L)	Time (min)	Conversion (%)	$M_n \times 10^{-5}$ (g/mol)	$M_w \times 10^{-5}$ (g/mol)
1	120	0.005	15	2.78 (3.05)	2.61 (1.84)	5.33 (3.58)
			60	13.05 (11.68)	2.17 (1.88)	4.27 (3.65)
			180	38.66 (33.03)	2.19 (1.99)	4.30 (3.88)
			240	42.58 (43.86)	2.39 (2.04)	4.57 (4.00)
			360	– (68.64)	2.28 (2.14)	4.46 (4.21)
2	120	0.01	15	4.35 (3.70)	2.32 (1.97)	3.60 (3.79)
			60	16.23 (14.30)	1.75 (2.01)	3.38 (3.87)
			180	42.14 (42.20)	2.00 (2.13)	3.81 (4.14)
			240	62.12 (58.32)	2.18 (2.19)	4.21 (4.27)
			360	92.05 (95.62)	2.50 (2.28)	5.32 (4.44)
3	120	0.02	15	3.83 (4.77)	2.23 (2.02)	4.30 (3.95)
			60	17.88 (18.47)	2.21 (2.05)	4.84 (3.98)
			180	55.16 (59.20)	1.94 (2.18)	3.65 (4.24)
			240	71.22 (87.39)	2.00 (2.23)	3.63 (4.34)
			360	98.22 (99.93)	1.74 (2.21)	3.16 (4.31)
4	130	0.01	15	4.42 (6.63)	1.86 (1.37)	3.52 (2.70)
			30	11.70 (13.26)	1.47 (1.39)	2.81 (2.73)
			45	20.04 (19.39)	1.41 (1.41)	2.61 (2.77)
			60	26.64 (25.53)	1.50 (1.42)	2.67 (2.81)
			90	40.48 (38.05)	1.47 (1.46)	2.67 (2.88)
			180	86.51 (82.94)	1.50 (1.55)	2.77 (3.08)
			240	98.10 (99.57)	1.57 (1.56)	3.30 (3.11)

The theoretical predictions are indicated in parentheses.

increased the reaction rates. The existence of an initiator concentration that yielded the highest molecular weights at a given polymerization temperature was also observed. An initiator concentration of 0.01 mol/L seemed to be optimal for obtaining high reaction rates and molecular weights at a reaction temperature of 120°C.
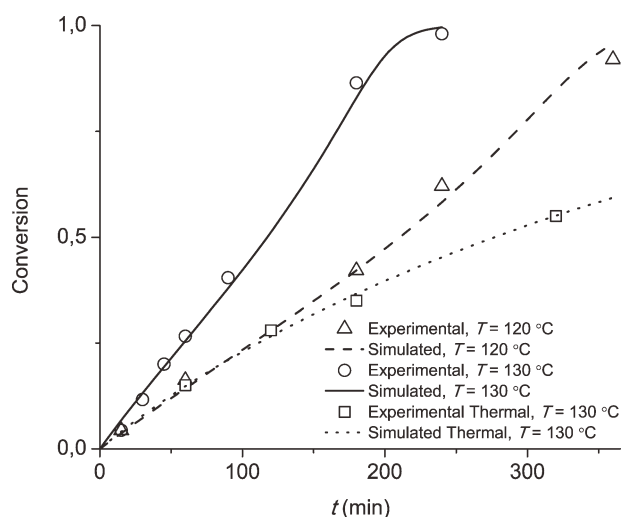
Figures 2 and 3 show the evolution of conversion and the average molecular weights for the reactions with a 0.01 mol/L concentration of DEKTP (experiments 2 and 4 in Table I). The evolution of conversion for the thermal polymerization of St is also presented in Figure 2 for comparison purposes (where T is the temperature and t is the time). As shown in Figure 2, an increase in R_p was observed as the temperature increased. For
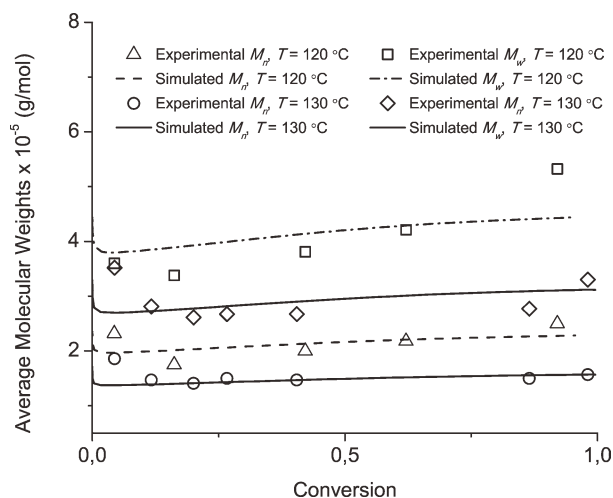

Figure 2. Conversion as a function of time for experiments 2 and 4 of Table I. The evolution of conversion for the St thermal polymerization at 130°C is also represented.

Figure 3. Average molecular weights as a function of conversion for experiments 2 and 4 from Table I.

Table II. Adopted Kinetic Mechanism

Initiation

Thermal initiation

$$3St \xrightarrow{k_i} 2S_1 \cdot^{(0)}$$

Chemical initiation

$$I^{(3)} \xrightarrow{3k_{d1}} \cdot I \cdot^{(2)}$$

$$\cdot I \cdot^{(2)} + St \xrightarrow{2k_{p1}} \cdot S_1 \cdot^{(2)}$$

Propagation ($n = 1, 2, 3, \ldots; i = 0, 1, 2, \ldots$)

$$S_n \cdot^{(i)} + St \xrightarrow{k_p} S_{n+1} \cdot^{(i)}$$

$$\cdot S_n \cdot^{(i)} + St \xrightarrow{2k_i} \cdot S_{n+1} \cdot^{(i)}$$

Transfer to monomer ($n = 1, 2, 3, \ldots; i = 0, 1, 2, \ldots$)

$$S_n \cdot^{(i)} + St \xrightarrow{k_{fM}} S_n^{(i)} + S_1 \cdot^{(0)}$$

$$\cdot S_n \cdot^{(i)} + St \xrightarrow{2k_{fm}} S_n \cdot^{(i)} + S_1 \cdot^{(0)}$$

Reinitiation ($n = 2, 3, \ldots; m = 1, 2, \ldots, n-1; i = 1, 2, \ldots;$ $j = 0, 1, 2, \ldots, i$)

$$S_n^{(i)} \xrightarrow{k_{d2}} S_{n-m} \cdot^{(i-j)} + S_m \cdot^{(j-1)} \cdot$$

Combination termination ($n, m = 1, 2, 3, \ldots; i, j = 0, 1, 2, \ldots$)

$$\cdot S_n \cdot^{(i)} + \cdot S_m \cdot^{(j)} \xrightarrow{4k_{tc}} \cdot S_{n+m} \cdot^{(i+j)}$$

$$\cdot S_n \cdot^{(i)} + \cdot S_m \cdot^{(j)} \xrightarrow{2k_{tc}} S_{n+m} \cdot^{(i+j)}$$

$$S_n \cdot^{(i)} + \cdot S_m \cdot^{(j)} \xrightarrow{k_{tc}} S_{n+m}^{(i+j)}$$

experiments 2 and 4, an inflection point in the conversion evolution curve was observed because of the sequential nature of the initiator decomposition. As expected, this inflection point did not appear in the case of purely thermal St polymerization. For the period of time evaluated, the molecular weights increased with the reaction (Figure 3). The calculated polydispersities were around 2; this was in agreement with reported results for multifunctional initiators.[1,9] As discussed in Cerna et al.,[11] these behaviors in the temperature range 120–130°C indicated that the initiator was decomposed by a sequential mechanism of decomposition of the peroxide sites, by which the diradicals formed by initiator decomposition had two undecomposed peroxide groups.

MATHEMATICAL MODEL

Kinetic Mechanism

The proposed kinetics involve the initiation via a symmetrical cyclic trifunctional initiator, thermal initiation, propagation, transfer to the monomer, combination termination, and reinitiation. The global kinetic mechanism is presented in Table II. The following was assumed:

1. At the temperature employed, the initiator decomposition was due exclusively to sequential decomposition.
2. Intramolecular termination was neglected.
3. Disproportion termination was negligible.
4. All peroxide groups present in the trifunctional initiator and in the accumulated polymer exhibited the same thermal stability.
5. Because of the short lifetime of radicals, the decomposition of undecomposed peroxide groups could not occur in radical molecules.

6. Propagation and transfer reactions were unaffected by the chain length or conversion.
7. Degradation reactions were negligible.

Note the following:

1. When two monoradicals with i and j undecomposed peroxide groups terminate, the formed polymer will contain $i + j$ undecomposed peroxide groups.
2. Diradicals only have an even number of peroxide groups, as they are generated only by propagation of the initiator diradical (with only two peroxide groups) and by the combination termination of other diradicals, all of which have an even number of peroxide groups.
3. Reinitiation involves the decomposition of a peroxide group within a polymer chain with undecomposed peroxide groups, which generates two monoradicals capable of further growth. Because of the molecular structure of the DEKTP molecule, only linear diradicals and monoradicals and linear polymer chains can be formed in the reaction system.

Homogeneous Model

From the kinetics of Table II and with the assumption of homogeneous bulk polymerization, the mathematical model discussed in the Appendix was developed. This model was based on the mass balances for the chemical species present in the reaction system. To model the reinitiation reactions, polymeric chains were assumed to have uniformly distributed peroxide groups. A random-chain scission could then be performed with a uniformly distributed random variable (see Appendix, Distribution Module).

The basic module in the Appendix allows the prediction of global chemical species' evolution along the reaction (total monoradicals and diradicals, total polymer). The distributions module in the Appendix allows simulation of the evolution of all chemical species characterized by their chain length and their number of undecomposed peroxide groups and allows the estimation of the evolution of the MWD of each species and the number of undecomposed peroxide groups.

The proposed model considers a constant temperature and assumes that the reactor cooling–heating system is ideal in the sense that it is capable of providing or removing the exact amount of heat needed to keep the temperature constant. However, it is possible to simulate reactions at different temperatures through the use of Arrhenius expressions for the kinetic coefficients. The gel effect was indirectly considered by appropriate reduction of the value of the termination kinetic coefficient with increasing conversion.[19]

The basic module is self-sufficient from the calculation point of view, and for its resolution, eqs. (A.1), (A.2), (A.5), (A.11), (A.12), (A.16), (A.23), and (A.25) must be simultaneously solved. The equations of the distributions module must be integrated with the basic module results.

The basic module is solved by a standard stiff differential equation numerical method based on a second-order modified Rosenbrock formula. In the distributions module, a large number of equations (>250,000) must be integrated. For this reason, an

Table III. Employed Kinetic Constants

k_d and k_{d2} (s^{-1})	$4.16 \times 10^8 \, e^{-25506/RT}$	Adjusted in this study
k_i (L^2 mol^{-1} s^{-1})	$1.1 \times 10^5 \, e^{-27340/RT}$	Peng,[21] Yoon and Choi[8]
k_{p1} and k_p (L mol^{-1} s^{-1})	$1.0 \times 10^7 \, e^{-7067/RT}$	Villalobos et al.[9]
k_{fM} (L mol^{-1} s^{-1})	$1.17 \times 10^{10} \, e^{-18651/RT}$	Adjusted in this study
k_{tc} (L mol^{-1} s^{-1})	$1.7 \times 10^9 \, e^{-(1667.3/RT)-2(C_1 x + C_2 x2 + C_3 x3)a}$	Friis and Hamielec[19]
f	0.98	Cerna[18]

$R = 1986$ cal mol^{-1} K^{-1}.
$^a C_1 = 2.75 - 0.00505T$; $C_2 = 9.56 - 0.0176T$; $C_3 = 3.03 + 0.00785T$.

explicit forward Euler method was used with the time intervals obtained from resolution of the basic module. A typical simulation requires less than 1 s for the basic module and about 15 min for the distribution module with an AMD Turion 64 based processor with 1.80 GHz.

SIMULATION RESULTS

The adopted kinetic parameters used for the simulation are presented in Table III.

The expressions for k_{d1} (kinetic coefficient for decomposition of a peroxide group in the initiator), k_{d2} (kinetic coefficient for decomposition of peroxide groups within the polymer chains), and k_{fM} (kinetic coefficient for transfer to monomer reactions) were adjusted in this work. Because peroxide groups in the polymer chains were assumed to have the same thermal stability as the peroxide groups in the initiator, $k_{d2} = k_{d1}$. Because of the short simulation times required, a fast interactive adjustment was possible. The adjusted values for k_{d1} were in agreement with the reported results for DEKTP decomposition in toluene.[11] The value k_{fM} was within the ranges reported for St polymerization.[20] The basic module allowed the adjustment for k_{d1} and k_{d2} from the estimation of the monomer conversion. The parameter k_{fM} was adjusted to fit the experimental data of the average molecular weights with the distributions module.

The expressions for k_p (kinetic coefficient for propagation reactions), k_{tc} (kinetic coefficient for combination termination reactions), and k_i (kinetic coefficient for thermal initiation reactions) were directly adopted from the literature,[7,9,19,21] and the value for f (initiator efficiency factor) was obtained from experimental results by Cerna et al.[18]

The model was used to simulate experiments 1–4 shown in Table I. The simulated results are compared with the experimental results in Table I and Figures 2 and 3. In general, very good agreement between the predicted and measured values was observed. Figures 2 and 3 show the simulation results corresponding to the evolution of the conversion and the average molecular weights for experiments 2 and 4 from Table I. The change of the slope in the conversion curve in Figure 2 at approximately 200 min at 120°C and 150 min at 130°C was due to the combined effect of the thermal and chemical initiators; this included initiator decomposition and decomposition of unreacted peroxide groups within the polymer chains, together with the gel effect, globally producing an increase in R_p. The reinitiation reactions within the polymer chains were also responsible for the high molecular weights observed experimen-

tally and predicted by the model, as the scission of polymer chains could generate long-chain monoradicals, which were capable of further growth by propagation reactions.

The mathematical model was also used to study the coupling effect of thermal and chemical initiation on R_p. In Figure 2, the experimental and simulated conversion curves for polymerizations carried out at 130°C in the absence of initiator are shown. The results indicate that at temperatures of 130°C, thermal polymerization contributed, on average, to about 60% of the total R_p.

Aside from the prediction of the experimental results presented in Table I and Figures 2 and 3, the model was used to simulate other variables. The model predictions are shown in Figures 4–7.

Figure 4 represents the evolution of R_p, as defined by eq. (A.2), as a function of time, which could be computed with the basic module of the Appendix. Figure 4 shows that around 200 min at 200°C and 150 min at 130°C, R_p increased as a result of chemical and thermal initiation, decomposition of peroxide groups within the formed polymer chains, and the gel effect, as explained for Figure 2. This increase in R_p was also be observed indirectly in the change of the slope of the conversion curve in Figure 2. The drop in the value of R_p around 300 min at 120°C and 200 min at 130°C was due to monomer depletion. For comparison purposes, the evolution of R_p in the absence of DEKTP initiation (i.e., a purely thermal polymerization) is also represented. It can be seen that R_p in this case was a monotonically decreasing function of time.
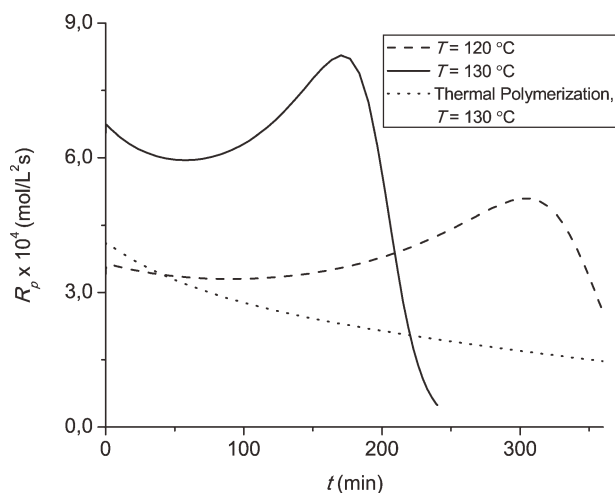

Figure 4. R_p as a function of time for experiments 2 and 4 from Table I. R_p for St thermal polymerization at 130°C is also shown.
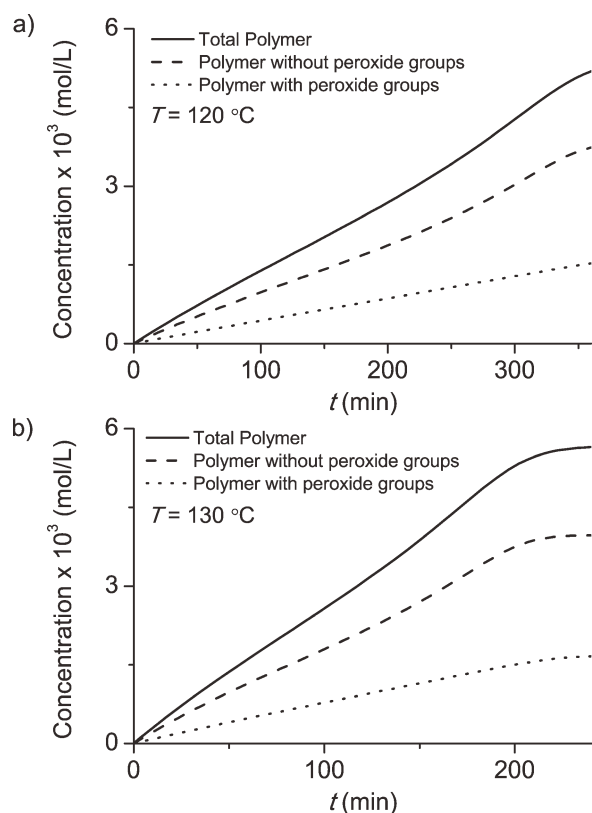
Figure 5. Evolution of total polymer, dead polymer, and total polymer with undecomposed peroxide groups for experiments (a) 2 and (b) 4 from Table I.

In Figure 5, the evolutions of the total polymer species' molar concentration are presented. The total polymer consisted of total dead polymer (i.e., without undecomposed peroxide groups) and total polymer with undecomposed peroxide groups. The dead polymer concentration monotonically increased with reaction time, exhibiting a slope that increased around 200 min at 120°C and 150 min at 130°C; this coincided with the time at which R_p increased (as indicated in Figures 2 and 4). The figure shows that the molar fraction of total polymer with undecomposed peroxide groups was close to 30%.

Figure 6 shows the evolutions of the different polymer species, characterized by the number of undecomposed peroxide groups within the polymeric chains. A logarithmic scale was used in the concentration axis to show the differences in magnitudes. Only polymer chains with one, two, three, four, five, six, and eight undecomposed peroxide groups are considered in the figure for clarity reasons. The evolution of the concentration of the different polymers species was highly dependent on the undecomposed peroxide group numbers because of the fact that peroxide groups in the polymer were a result of the propagation, transfer, and termination of diradicals generated by initiator decomposition but also by the decomposition of polymeric chains with a higher peroxide group number. A great number of monoradicals without peroxide groups was also produced by the thermal initiation of the monomer at 120 and 130°C, and as a result, dead polymer was the most abundant polymer species. It was possible to observe that the

molar concentration of the polymer decreased with increasing peroxide group number per chain when we considered polymers with an even number of peroxide groups. The same could be stated for polymers with an odd number of peroxide groups. For polymers with an even number of peroxide groups, the concentrations showed a similar evolution; this indicated that most of the peroxide groups in the polymer chains were generated by initiator decomposition. This was not the case for polymers with an odd number of peroxide groups because radicals with an odd number of peroxide groups were generated only by decomposition reactions. For this reason, polymers with an odd number of undecomposed peroxide groups were formed in the reaction system later than polymers with an even number of peroxide groups. These types of behaviors were a clear result of the sequential decomposition of the initiator molecule. The increase in polymer concentration for high peroxide group numbers (>3) at high reaction times could be explained as follows: when the conversion was close to a value of 1, little monomer was left for the thermal initiation reactions. However, the initiator decomposition was still important, and all of the radicals generated had two undecomposed peroxide groups. The reinitiation reactions also generated radicals with undecomposed peroxide groups, and polymer generation was mostly done by termination reactions between these radicals. These factors resulted in an increase in the concentration of the polymer with a high number of undecomposed peroxide groups toward the end of the polymerization.
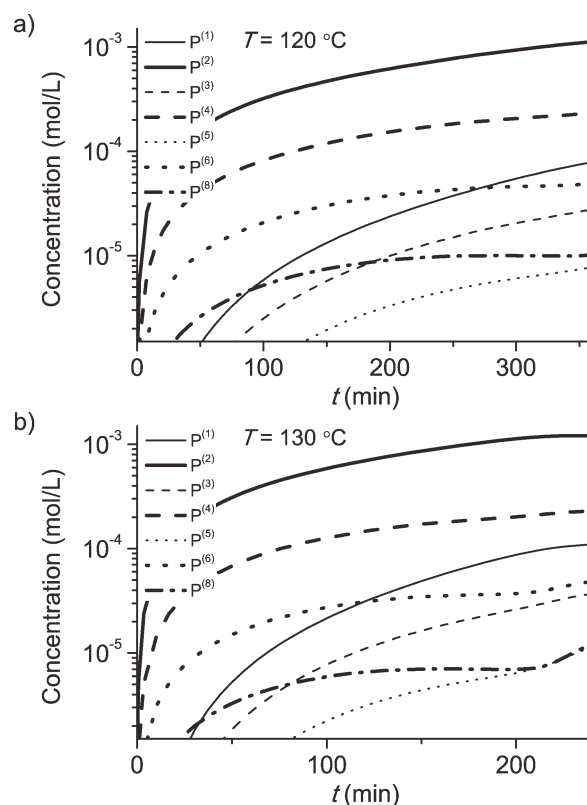

Figure 6. Evolution of the total polymeric species characterized by the number of undecomposed peroxide groups for experiments (a) 2 and (b) 4 from Table I.
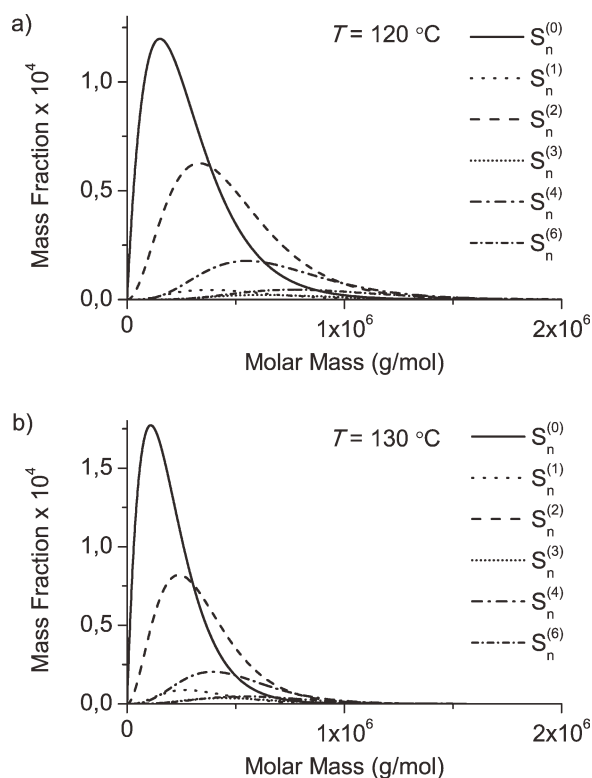
Figure 7. MWDs of the polymeric species at the end of polymerization for experiments (a) 2 and (b) 4 from Table I.

Figure 7 shows the MWDs of the formed polymer species at the end of the polymerization reaction. Only the MWDs of a few polymeric species are represented to keep the picture clear but still representative. The obtained MWDs showed that polymers with a high number of undecomposed peroxide groups had a wider distribution over higher molecular weights. This was consistent with the fact that high peroxide group numbers arose from a termination combination or the transfer of monoradicals that were generated by the diradicals of initiator decomposition. These diradicals could propagate before terminating, so it was expected that termination of two diradicals would generate a long-chain monoradical, which could itself terminate with another long-chain monoradical. As expected, polymer chains with one undecomposed peroxide group were, on average, shorter that the ones from the polymer with two undecomposed peroxide groups because the former was generated mostly by decomposition of the latter after transfer to the monomer or termination with a radical without peroxide groups. Polymers with a greater number of peroxide groups had a relatively low mass fraction but enough to significantly increase the average molecular weight. Through comparison of the MWDs obtained at different temperatures, it was possible to see that lower temperatures tended to increase the mass fraction of the polymer with undecomposed peroxide groups compared to the total polymer.

In Table IV, the effect of initiator concentration on the average molecular weight is theoretically evaluated. The model allowed us to calculate the average molecular weights for total conversion as a function of the initial initiator concentration. The simulated results indicate that at a given reaction temperature, there was an initiator concentration that yielded the maximum values of the average molecular weights; this indicated the presence of an optimum initiator concentration. This fact was also observed experimentally at 120°C, as shown in Table I in experiments 1–3. The existence of this optimum could be interpreted as follows: at low initiator concentration, a low proportion of diradicals was generated by initiator decomposition. As these radicals propagated before generating a monoradical, which was capable of further propagation, the effect on the average molecular weight was less significant. An increase in the initiator concentration increased the proportion of diradicals, and this results in an increase in the average molecular weight. At high initiator concentrations, the dominating effect was the large number of active sites in the system (by both chemical and thermal initiation). This resulted in shorter polymer chains and lower average molecular weights. The value of this optimum concentration depended on the polymerization temperature, which also modified R_P. For polymerization temperatures of 120–130°C the optimum concentration was found to be 0.01 mol/L.

As shown, the proposed mathematical model allowed us to predict the concentration and MWD values of the polymer species with undecomposed peroxide groups at the end of the polymerization reaction. These variables could be used to study the evolution of the polymer structure over the course of postpolymerization processes carried out at high temperatures (e.g., devolatilization), where the decomposition of the remaining peroxide groups could take place and, thereby, modify the values of the final properties (processing and mechanical properties).

To estimate the decrease in the molecular weights due to decomposition of the remaining peroxide groups, the model was used to simulate the evolution of a polymer (obtained at 130°C and with an initial DEKTP concentration of 0.01 mol/L) subjected to a process at temperatures of 180–200°C with a residence time of 25 min. These values for the temperature and residence time are typical values for a devolatilization

Table IV. Theoretical Study of the Effects of the Initial Initiator Concentration on the Average Molecular Weights at Total Conversion for Temperatures of 120 and 130°C

	$T = 120°C$		$T = 130°C$	
$[I^{(3)}]$ (mol/L)	$M_n \times 10^{-5}$ (g/mol)	$M_w \times 10^{-5}$ (g/mol)	$M_n \times 10^{-5}$ (g/mol)	$M_w \times 10^{-5}$ (g/mol)
0.001	2.14	4.22	1.50	2.99
0.002	2.16	4.26	1.53	3.07
0.005	2.22	4.36	1.56	3.11
0.01	2.28	4.44	1.57	3.11
0.02	2.21	4.31	1.56	3.08
0.05	2.12	4.02	1.49	2.86

process.[22] The simulation results indicated decreases in the molecular weights of about 30–40%, depending on process temperature. These results should be only considered to be estimates, as the model did not include high-temperature degradation reactions. In addition, to compare the performance of this initiator and that of a bifunctional initiator in an industrial polymerization process and the effect on the final average molecular weights, we need consider not only the polymerization reaction stage but also the downstream postreaction stages for which the model developed in this work might not be appropriate.

CONCLUSIONS

In this study, we experimentally and theoretically investigated the use of the symmetrical trifunctional initiator DEKTP in the bulk polymerization of St. The experimental work consisted of a series of isothermal batch polymerizations at different temperatures, in which the conversion and average molecular weights were determined. For the theoretical analysis, a new mathematical model was developed that allowed us to simulate the evolution of the chemical species characterized by the number of undecomposed peroxide groups within the chains, including diradicals and monoradicals and polymeric species. We accounted for reinitiation reactions with a uniformly distributed random variable to simulate random-chain scission.

The main result was that the use of DEKTP allowed us to obtain high R_p's and high molecular weights simultaneously because of its sequential decomposition. This led to the formation of diradicals and monoradicals with undecomposed peroxide groups. These peroxide groups were then found in the polymeric chains, which were susceptible of reinitiation. The simulation of the proposed kinetic mechanism provided values that were in very good agreement with the experimental results.

For a given polymerization temperature, the experimental and simulation results showed the existence of an optimum initiator concentration, for which the produced average molecular weights were highest.

The fact that undecomposed peroxide groups remained within the polymer chains is an important issue that should be taken into consideration for an industrial polymerization process. Simulation of the complete polymerization process would require an extension of the model to continuous polymerization processes and its modification to account for high-temperature reactions and other phenomena that could alter the polymer molecular structure during downstream postreaction processes.

In future studies, the kinetic mechanism could be extended to include the total decomposition of the initiator molecule at higher reaction temperatures, and a generic model for multifunctional initiators could also be developed. The mathematical model could also be extended to continuous systems and applied to control polymer properties in an industrial production process.

REFERENCES

1. Choi, K. Y.; Lei, G. D. *AIChE J.* **1987,** *33*, 2067.
2. Estenoz, D. A.; Leal, G. P.; López, Y. R.; Oliva, H. M.; Meira, G. R. *J. Appl. Polym. Sci.* **1996,** *62*, 917.
3. Kim, J.; Liang, W.; Choi, K. *Ind. Eng. Chem. Res.* **1989,** *28*, 131.
4. Priddy, D. B. *Adv Polym Sci* **1994,** *111*, 67.
5. Drumright, R. E.; Kastl, P. E.; Priddy, D. B. *Macromolecules* **1993,** *26*, 2246.
6. González, I. M.; Meira, G. R.; Oliva, H. *J. Appl. Polym. Sci.* **1996,** *59*, 6.
7. Yoon, W. J.; Choi, K. Y. *J. Appl. Polym. Sci.* **1992,** *46*, 1353.
8. Yoon, W. J.; Choi, K. Y. *Polymer* **1992,** *33*, 4582.
9. Villalobos, M. A.; Hamielec, A. E.; Wood, P. E. *J. Appl. Polym. Sci.* **1991,** *42*, 629.
10. Choi, K. Y.; Liang, W. R.; Lei, G. D. *J. Appl. Polym. Sci.* **1988,** *35*, 1547.
11. Cerna, J.; Morales, G.; Eyler, G. N.; Canizo, A. I. *J. Appl. Polym. Sci.* **2002,** *83*, 1.
12. Cavin, L.; Rouge, A.; Meyer, T.; Renken, A. *Polymer* **2000,** *41*, 3925.
13. Mateo, C. M.; Eyler, G. N.; Alvarez, E. E.; Cañizo, A. I. *Inf. Tecnol.* **1998,** *9*(2), 19.
14. Scorah, M. J.Ph.D. Thesis, University of Waterloo, **2005.**
15. Scorah, M. J.; Dhib, R.; Penlidis, A. *Chem. Eng. Sci.* **2006,** *61*, 4827.
16. Sheng, W. C.; Wu, J. Y.; Shan, G. R.; Huang, Z. M.; Weng, Z. X. *J. Appl. Polym. Sci.* **2004,** *94*, 1035.
17. Eyler, N.; Cañizo, A. I.; Alvarez, E. E.; Cafferata, L. F. R. *Tetrahedr. Lett.* **2003,** *34*, 1745.
18. Cerna, J. Ph.D. Thesis, Centro de Investigaciones en Química Aplicada, **2002.**
19. Friis, N.; Hamielec, A. E. *Am. Chem. Soc. Symp. Ser.* **1976,** *24*, 82.
20. Meyer, T.; Keurentjes, J.Handbook of Polymer Reaction Engineering; Wiley:New York, **2005.**
21. Peng, F. M. *J. Appl. Polym. Sci.* **1990,** *40*, 1289.
22. Estenoz, D. A.; Gómez, N.; Oliva, H. M.; Meira, G. R. *AIChE J.* **1998,** *44*, 427.

APPENDIX

Basic Module
Balances for the Nonpolymeric Reagents and Products
Initiator (DEKTP).

$$\frac{d}{dt}\left([I^{(3)}]V\right) = -3k_{d1}[I^{(3)}]V \qquad (A.1)$$

where $[I^{(3)}]$ is the trifunctional initiator concentration and V is the reaction volume.

Monomer. With the assumption of long-chain approximation (by which propagation is the only monomer-consuming reaction), one can write:

$$\frac{d}{dt}\left([St]V\right) = -R_p V = -k_p [St]\left([R\cdot] + 2[\cdot R\cdot]\right)V \qquad (A.2)$$

where R_p is the global St polymerization rate and

$$[R\cdot] = \sum_{i=0}^{\infty}\sum_{n=1}^{\infty}\left[S_n\cdot^{(i)}\right] \qquad (A.3)$$

$$[\cdot R\cdot] = \sum_{i=0}^{\infty}\sum_{n=1}^{\infty}\left[\cdot S_n\cdot^{(i)}\right] \qquad (A.4)$$

where $[S_n\cdot^{(i)}]$ is the concentration of PS monoradical of chain length n containing i undecomposed peroxide groups. Equations (A.3) and (A.4) represent the total concentrations of monoradicals and diradicals, respectively.

Radical Species. When we consider the mass balances of all free radicals appearing in the global kinetics, such balances provide the following:

$$\frac{d}{dt}\left([\cdot I\cdot^{(2)}]V\right) = \left(3fk_{d1}[I^{(3)}] - 2k_{p1}[\cdot I\cdot^{(2)}][St]\right)V \qquad (A.5)$$

$$\frac{d}{dt}\left([S_1\cdot^{(0)}]V\right) = \left\{2k_i[St]^3 - \left(k_p[S_1\cdot^{(0)}] - k_{fM}\left([R\cdot] + 2[\cdot R\cdot]\right)\right.\right.$$
$$\left.\left. + k_{fM}[S_1\cdot^{(0)}]\right)[St] - k_{tc}[S_1\cdot^{(0)}]\left([R\cdot] + 2[\cdot R\cdot]\right)\right\}V \quad (A.6)$$

$$\frac{d}{dt}\left([\cdot S_1\cdot^{(2)}]V\right) = \left\{\left(2k_{p1}[\cdot I\cdot^{(2)}] - 2k_p[\cdot S_1\cdot^{(2)}] - 2k_{fM}[\cdot S_1\cdot^{(2)}]\right)[St]\right.$$
$$\left. - 2k_{tc}[\cdot S_1\cdot^{(2)}]\left([R\cdot] + 2[\cdot R\cdot]\right)\right\}V \quad (A.7)$$

$$\frac{d}{dt}\left([\cdot S_n\cdot^{(i)}]V\right) = \left\{2k_p[St]\left([\cdot S_{n-1}\cdot^{(i)}] - [\cdot S_n\cdot^{(i)}]\right)\right.$$
$$- 2k_{fM}[St][\cdot S_n\cdot^{(i)}] - 2k_{tc}\left([R\cdot] + 2[\cdot R\cdot]\right)[\cdot S_n\cdot^{(i)}]$$
$$\left. + 2k_{tc}\sum_{j=0}^{i}\sum_{m=1}^{n-1}[\cdot S_{n-m}\cdot^{(i-j)}][\cdot S_m\cdot^{(j)}]\right\}V \quad (n \geq 2, i = 2, 4, 6...) \quad (A.8)$$

$$\frac{d}{dt}\left([S_n\cdot^{(i)}]V\right) = \left\{\left(k_p\left([S_{n-1}\cdot^{(i)}] - [S_n\cdot^{(i)}]\right)\right.\right.$$
$$+ k_{fM}\left(2[\cdot S_n\cdot^{(i)}] - [S_n\cdot^{(i)}]\right)[St] - k_{tc}\left([R\cdot] + 2[\cdot R\cdot]\right)[S_n\cdot^{(i)}]$$
$$+ 2k_{tc}\sum_{j=0}^{i}\sum_{m=1}^{n-1}[\cdot S_{n-m}\cdot^{(i-j)}][S_m\cdot^{(j)}]$$
$$\left. + k_{d2}\sum_{j=i+1}^{\infty}\sum_{m=n+1}^{\infty}p_{mj}(n,i)j[S_m^{(j)}]\right\}V \quad (n \geq 2, i = 0, 1, 2, 3...) \quad (A.9)$$

where $[\cdot I\cdot^{(2)}]$ is the concentration of the initiator diradical with two undecomposed peroxide groups, $[S_1\cdot^{(0)}]$ is the concentration of the monomer monoradical without undecomposed peroxide groups, $[S_1\cdot^{(2)}]$ is the concentration of the monomer diradical with two undecomposed peroxide groups, $[S_n\cdot^{(i)}]$ is the concentration of the PS diradical of chain length n containing i undecomposed peroxide groups, and $p_{mj}(n,i)$ is the probability that the scission of a chain of dead polymer of length m and j peroxide groups yields a monoradical of chain length n with i peroxide groups. When this probability is added over all is and ns, the following can be proven:

$$\sum_{i=1}^{\infty}\sum_{n=1}^{\infty}\sum_{j=i+1}^{\infty}\sum_{m=n+1}^{\infty}p_{mj}(n,i)j[S_m^{(j)}] = 2\sum_{i=1}^{\infty}\sum_{n=1}^{\infty}i[S_n^{(i)}] = 2[Pe_P] \qquad (A.10)$$

where $[Pe_P]$ is the concentration of peroxide groups in the polymer chains. The 2 in eq. (A.10) arises from the fact that the scission of any polymer chain with peroxide groups produces two monoradicals.

From eqs. (A.6) through (A.10), the total concentration of monoradicals and diradicals may be obtained:

$$\frac{d}{dt}\left([R\cdot]V\right) = \left\{2k_i[St]^3 + 4k_{fM}[St][\cdot R\cdot] - k_{tc}[R\cdot]^2 + 2k_{d2}[Pe_P]\right\}V \qquad (A.11)$$

$$\frac{d}{dt}\left([\cdot R\cdot]V\right) = \left\{\left(2k_{p1}[\cdot I\cdot^{(2)}] - 2k_{fM}[\cdot R\cdot]\right)[St]\right.$$
$$\left. - 2k_{tc}[\cdot R\cdot]\left([R\cdot] + 2[\cdot R\cdot]\right) + 2k_{tc}[\cdot R\cdot]^2\right\}V \quad (A.12)$$

Balances for the Polymeric Species
Polymer without peroxide groups (i = 0).

$$\frac{d}{dt}\left([S_n^{(0)}]V\right) = \left\{k_{fM}[St][S_n\cdot^{(0)}] + \frac{k_{tc}}{2}\sum_{m=1}^{n-1}[S_{n-m}\cdot^{(0)}][S_m\cdot^{(0)}]\right\}V \quad (n \geq 2) \qquad (A.13)$$

Polymer with peroxide groups (i ≠ 0).

$$\frac{d}{dt}\left([S_n^{(i)}]V\right) = \left\{k_{fM}[St][S_n\cdot^{(i)}] + \frac{k_{tc}}{2}\sum_{j=0}^{i}\sum_{m=1}^{n-1}[S_{n-m}\cdot^{(i-j)}][S_m\cdot^{(j)}]\right.$$
$$\left. - k_{d2}i[S_n^{(i)}]\right\}V \quad (n \geq 2, i = 1, 2, 3...) \quad (A.14)$$

The concentration of the polymer with i undecomposed peroxide groups $\{[P^{(i)}]\}$ can be defined as follows:

$$[P^{(i)}] = \sum_{n=1}^{\infty}[S_n^{(i)}] \qquad (A.15)$$

Let us define the total polymer concentration $([P])$:

$$[P] = \sum_{i=0}^{\infty}[P^{(i)}] = \sum_{i=0}^{\infty}\sum_{n=1}^{\infty}[S_n^{(i)}] \qquad (A.16)$$

Through the addition of eq. (A.13) over all ns and eq. (A.14) over all ns and all is, the balance for the molar concentration of polymer can be written as follows:

$$\frac{d}{dt}\left([P]V\right) = \left\{k_{fM}[St][R\cdot] + \frac{k_{tc}}{2}[R\cdot]^2 - k_{d2}[Pe_P]\right\}V \qquad (A.17)$$

Peroxide Groups. The total concentration of peroxide groups is as follows:

$$[Pe] = 3[I^{(3)}] + 2[\cdot I\cdot^{(2)}] + [Pe_{R\cdot}] + [Pe_{\cdot R\cdot}] + [Pe_P] \qquad (A.18)$$

with

$$[\text{Pe}_{\text{R}\cdot}] = \sum_{i=1}^{\infty} \sum_{n=1}^{\infty} i [\text{S}_n\cdot^{(i)}] \tag{A.19}$$

$$[\text{Pe}_{\cdot\text{R}\cdot}] = \sum_{i=1}^{\infty} \sum_{n=1}^{\infty} i [\cdot\text{S}_n\cdot^{(i)}] \tag{A.20}$$

$$[\text{Pe}_{\text{P}}] = \sum_{i=1}^{\infty} \sum_{n=1}^{\infty} i [\text{S}_n^{(i)}] \tag{A.21}$$

where $[\text{Pe}_{\text{R}\cdot}]$, $[\text{Pe}_{\cdot\text{R}\cdot}]$, and $[\text{Pe}_{\text{P}}]$ represent the molar concentration of peroxide groups accumulated in the monoradicals, diradicals, and polymer species. From eq. (A.18) and with the assumption of a pseudo-steady state for radical species (by which all time derivatives may be set to zero), the following can be written:

$$\frac{d[\text{Pe}]}{dt} = 3\frac{d[\text{I}^{(3)}]}{dt} + \frac{d[\text{Pe}_{\text{P}}]}{dt} \tag{A.22}$$

Peroxide groups are consumed only by decomposition reactions in the initiator and the polymer chains. Therefore

$$\frac{d[\text{Pe}]}{dt} = -3k_{d1}[\text{I}^{(3)}] - k_{d2}[\text{Pe}_{\text{P}}] \tag{A.23}$$

Through consideration of eqs. (A.1) and (A.23) and from eq. (A.22), the total peroxide groups contained in the polymer chains can be calculated from the following equation:

$$\frac{d[\text{Pe}_{\text{P}}]}{dt} = 6k_{d1}[\text{I}^{(3)}] - k_{d2}[\text{Pe}_{\text{P}}] \tag{A.24}$$

Conversion. The monomer conversion can be calculated from the following:

$$x = \frac{[\text{St}]^0 V^0 - [\text{St}] V}{[\text{St}]^0 V^0} \tag{A.25}$$

where the superscript 0 indicates initial conditions. In this model, we neglect the effect of volume contraction and therefore

$$x = \frac{[\text{St}]^0 - [\text{St}]}{[\text{St}]^0} \tag{A.26}$$

Equations (A.1), (A.2), (A.5), (A.11), (A.12), (A.17), (A.24), and (A.26) can be simultaneously solved to determine the evolutions of $[\text{I}]$, $[\cdot\text{I}\cdot^{(2)}]$, $[\text{St}]$, $[\text{R}\cdot]$, $[\cdot\text{R}\cdot]$, $[\text{P}]$, $[\text{Pe}_{\text{P}}]$, and x.

Distributions Module

Consider eqs. (A.8) and (A.9). With a pseudo-steady state assumed, all time derivatives can be set to zero and the following recurrence formulas can be obtained:

$$[\cdot\text{S}_n\cdot^{(i)}] = \frac{k_p[\text{St}][\cdot\text{S}_{n-1}\cdot^{(i)}] + k_{tc}\sum_{j=1}^{i}\sum_{m=1}^{n-1}[\cdot\text{S}_{n-m}\cdot^{(i-j)}][\cdot\text{S}_m\cdot^{(j)}]}{k_p[\text{St}] + k_{fM}[\text{St}] + k_{tc}([\text{R}\cdot] + [\cdot\text{R}\cdot])}$$
$$(n \geq 2, i = 2, 4, 6 \ldots) \tag{A.27}$$

$$[\text{S}_n^{(i)}\cdot] = \frac{\left(k_p[\text{S}_{n-1}\cdot^{(i)}] + 2k_{fM}[\cdot\text{S}_n\cdot^{(i)}]\right)[\text{St}] + 2k_{tc}\sum_{j=0}^{i}\sum_{m=1}^{n-1}[\cdot\text{S}_{n-m}\cdot^{(i-j)}][\text{S}_m\cdot^{(j)}]}{k_p[\text{St}] + k_{fM}[\text{St}] + k_{tc}([\text{R}\cdot] + 2[\cdot\text{R}\cdot])}$$
$$+ \frac{k_{d2}\sum_{j=i+1}^{\infty}\sum_{m=n+1}^{\infty}p_{mj}(n,i)j[\text{S}_m^{(j)}]}{k_p[\text{St}] + k_{fM}[\text{St}] + k_{tc}([\text{R}\cdot] + 2[\cdot\text{R}\cdot])} \qquad (n \geq 2, i = 0, 1, 2, 3 \ldots) \tag{A.28}$$

We define the following molar ratio

$$\sigma_2 = \frac{[\cdot\text{S}_1^{(2)}\cdot]}{[\text{R}\cdot] + 2[\cdot\text{R}\cdot]} \tag{A.29}$$

and the following dimensionless kinetic parameters:

$$\tau = \frac{k_{fM}}{k_p} \tag{A.30}$$

$$\beta = \frac{k_{tc}R_p}{(k_p[\text{St}])^2} = \frac{k_{tc}([\text{R}\cdot] + 2[\cdot\text{R}\cdot])}{k_p[\text{St}]} \tag{A.31}$$

$$\alpha = \tau + \beta \tag{A.32}$$

$$\gamma = \frac{k_{d2}}{k_p} \tag{A.33}$$

By replacing the definitions in eqs. (A.29), (A.30), (A.31), and (A.32) in eq. (A.27) and solving the recurrence formula, we can obtain following explicit expression for diradical MWD:

$$[\cdot\text{S}_n^{(2k)}\cdot] = \frac{1}{(1+\alpha)^{n-1}}(\beta\sigma_2)^{k-1}\frac{(n+k-2)!}{(n-k)!k!(k-1)!}[\cdot\text{S}_1^{(2)}\cdot]$$
$$(n \geq 2, k = 1, 2, 3 \ldots) \tag{A.34}$$

Equation (A.28) can then be written as follows

$$[\text{S}_n^{(i)}\cdot] = \frac{1}{1+\alpha}\left([\text{S}_{n-1}\cdot^{(i)}] + 2\tau[\cdot\text{S}_n\cdot^{(i)}]\right.$$
$$\left. + \frac{2\beta}{[\text{R}\cdot] + 2[\cdot\text{R}\cdot]}\sum_{j=0}^{i}\sum_{m=1}^{n-1}[\cdot\text{S}_{n-m}\cdot^{(i-j)}][\text{S}_m\cdot^{(j)}] + \frac{\gamma}{[\text{St}]}\Psi(n,i)\right)$$
$$(n \geq 2, i = 1, 2, 3 \ldots) \tag{A.35}$$

where

$$\Psi(n,i) = \sum_{j=i+1}^{\infty}\sum_{m=n+1}^{\infty}p_{mj}(n,i)j[\text{S}_m^{(j)}] \tag{A.36}$$

Equations (A.34) and (A.35) must be solved with eqs. (A.6) and (A.7). The number chain length distribution for the PS species can then be found by the integration of eqs. (A.13) and (A.14) with the expressions found for $[S_n^{(i)} \cdot]$.

The maximum chain length (with a maximum value of n) and number of peroxide groups (with a maximum value of i) simulated by resolution of the model were determined as follows: simulations were carried out with a large number for maximum undecomposed peroxide groups within the polymer chains (≤ 30) and a very large number for maximum chain length ($\leq 25{,}000$ monomer units). The maximum chain length and number of peroxide groups simulated was then adapted to ensure that the system simulated the species that determined the molecular structure of the polymer and the average molecular weights values and, at the same time, minimized the time required for the simulations.

To account for the formation of monoradicals from random scission of the polymer chains containing peroxide groups, we consider a polymer chain with length n and i peroxide groups, all of which have the same thermal stability.

Let m be a uniformly distributed random variable whose value ranges from 1 to $n - 1$. The polymer chain may form two monoradicals, one with length m and the other one with length $n - m$. These chains have $i - j$ and $j - 1$ undecomposed peroxide groups, respectively.

If the peroxide groups are uniformly distributed in the formed monoradicals, the following relation must hold:

$$\frac{j - 1}{n - m} = \frac{i - j}{m} \tag{A.37}$$

Therefore

$$j = \left[\frac{i(n - m) + m}{n} \right] \tag{A.38}$$

where the brackets indicate the integer part of the expression. The scission has then generated two monoradicals, one with length m and $i - j$ peroxide groups and the other one with length $n - m$ and $j - 1$ peroxide groups.

This scission must be performed for all polymer chains whose peroxide group number is greater than 0.

Average Molecular Weights. The number-average molecular weight (M_n) can be calculated with the following expression:

$$M_n = M_{St} \frac{\sum\limits_{i=0}^{\infty} \sum\limits_{n=2}^{\infty} n \left[S_n^{(i)} \right]}{\sum\limits_{i=0}^{\infty} \sum\limits_{n=2}^{\infty} \left[S_n^{(i)} \right]} \tag{A.39}$$

The weight-average molecular weight (M_w) can be calculated as follows:

$$M_w = M_{St} \frac{\sum\limits_{i=0}^{\infty} \sum\limits_{n=2}^{\infty} n^2 \left[S_n^{(i)} \right]}{\sum\limits_{i=0}^{\infty} \sum\limits_{n=2}^{\infty} n \left[S_n^{(i)} \right]} \tag{A.40}$$